



**SYNTHESIS AND CHARACTERIZATION OF
 $Ba_{0.5} Sr_{0.5} (CO_{0.8}Fe_{0.2})_{1-x} Ti_x O_{3-\delta}$ (BSCFTi) & $Ba_{0.5} Sr_{0.5} (CO_{0.8}Fe_{0.2})_{1-x} Zr_x O_{3-\delta}$ (BSCFZr)
CATHODES BY SOL-GEL PROCESS FOR SOLID OXIDE FUEL CELL**

**D.RAMAKRISHNA SHARMA^{A*}, Dr P.VIJAY BHASKAR RAO^B, M.NARSIMHA REDDY^C,
D.SRIKANTH^D**

^a Head, Department of physics, Visvesvaraya College of Engineering And Technology, Patelguda, Ibrahimpatnam, Hyderabad.T.S, India. mail id: dhulipalarks@gmail.com

^b Department of physics, St. Mary Engineering College, Deshmukhi(v), Nalgonda(dist), Telangana

^c Department of physics, N.M.R Engineering college Ghatkesar, R.R (Dist.), Telangana, India

ABSTRACT

The BSCFTi, Barium Strontium Cobalt Iron Titanate $\{Ba_{0.5}Sr_{0.5} (CO_{0.8} Fe_{0.2})_{1-x} Ti_x O_{3-\delta}\}$ and BSCFZr, Barium Strontium Cobalt Iron Zirconate $\{Ba_{0.5}Sr_{0.5} (CO_{0.8} Fe_{0.2})_{1-x} Zr_x O_{3-\delta}\}$ [Where δ is the deficiency of oxygen & x is various compositions] cathode powders have been synthesized by sol-Gel process using nitrate based powdered chemicals for SOFC applications as these powders are more useful for Cathodes for SOFCs. To obtain the low potential cathode materials suitable, SOL-GEL method is used and nano powders are prepared, kept for calcinations at $900^{\circ}C$ for 16 hr and at $1070^{\circ}C$ for about 6 hr. These were characterized by XRD, SEM with EDAX, and ionic conductivity is studied.

Keywords: SEM/EDAX, TGA/DSC; XRD; Density; $Ba_{0.5} Sr_{0.5} (CO_{0.8}Fe_{0.2})_{1-x} Ti_x O_{3-\delta}$

1. INTRODUCTION:

SOFC's (Solid oxide fuel cells) are one of the important energy devices with high oxygen vacancies. BSCF proved as good materials for solid cathode with appealing properties like ionic conductivity, super conductivity, Ferro electricity, etc., Various cathodes were used in LSM, SSC, LSCF, BSCF, etc., but, the thermo-mechanical suitability between electrolyte and cathode can be improved by mixing cathode material with new element or a small impurity. Such composite cathode will have a better ionic conductivity. As the cathode over potential is significant in SOFC's, it can be reduced by adding Titanium and Zirconium separately to BSCF. By increasing the percentage of Ti and Zr separately in site 'B' of ABO_3 (Perovskite structure), In this, oxygen ion vacancies will be pronounced along $(B^{3+/4+})-O^{2-}-(B^{3+/4+})$, due to overlapping of the oxygen p-orbital and transition-metal d-orbital. When Ba is in site 'A', it increases the amount of B^{4+} ions and increases oxygen vacancies and one can increase the efficiency and conductivity. There are various models developed to explain reaction mechanisms of cathodes, of SOFCs [9, 10]. Out of various fuel cells, solid-oxide fuel cells (SOFCs) have the benefit of eco friendly power generation with fuel [15] flexibility. SOFCs [16] have been designed and developed and cathodes are prepared by using BSCF(BaSrCoFe) newly, which exhibit high power densities i.e., $1,010mW/cm^2$ and $402mW/cm^2$ at $600^{\circ}C$ and $500^{\circ}C$ than conventional cells. In this Hydrogen is used as fuel and air as cathode gas. BSCFs are suitable for single chamber fuel cell operation. Hence, the alternative Perovskite Cathodes are chosen for high activity oxygen reduction. SOFCs will have high oxygen diffusivity. The important requirements for SOFC cathode materials are i) High electronic conductivity ii) Chemically suitable with electrolyte, iii) Stable in oxidation, iv) Large triple phase boundary, v) High ionic conductivity, vi) Suitable thermal expansion coefficient, vii) Simple fabrication and Low cost. There are many materials which explain the reaction mechanisms of SOFC. But, BSCF cathode preparation doped with Titanium and the over potential study is an important factor such that there will be rapid movement of oxygen ions [23]. This can also be obtained by increasing the porosity of BSCF cathode [24] which provide more dispersion of gases increasing

reduction of oxygen. Hence, the current density will be generated within the cell cathodes, like transport of oxygen, electrode kinetics, and involvement of chargeable particles in electrochemical processes.

In recent works, Itoh et.al has shown the presence of both covalent and ionic bonds in BSCFO_{3-δ} and increases electron and oxygen ion conductivity at fairly low values of temperature. This clearly explains that the stoichiometry of oxygen decreases with increase in temperature and hence reduction in cations in site 'B' [17, 18]. SOFC performance will purely depend on sample preparation, its reactants, chemicals, stoichiometry, calcinations, sintering, acids, and bases. In recent papers, it is suggested that, varying x and δ values in the BSCFO_{3-δ} [5582] will affect the performance. In the present paper, the objective is to prepare a cathode suitable for SOFC in single chamber fuel cell conditions. Hence, materials with a small percentage of Ti and Zr (with increasing values) are prepared separately and their characterization/values are compared. Hence, in the present study, investigation has been done with Ba_{0.5} Sr_{0.5} (CO_{0.8}Fe_{0.2})_{1-x}Ti_xO_{3-δ} (BSCFTi) & Ba_{0.5} Sr_{0.5} (CO_{0.8}Fe_{0.2})_{1-x}Zr_xO_{3-δ} (BSCFZr) by taking δ=0, δ=1 and x=0, 0.10, 0.15, 0.20, with different thermal properties. BSCF has proved as a good material for solid oxide [20,21,and22].

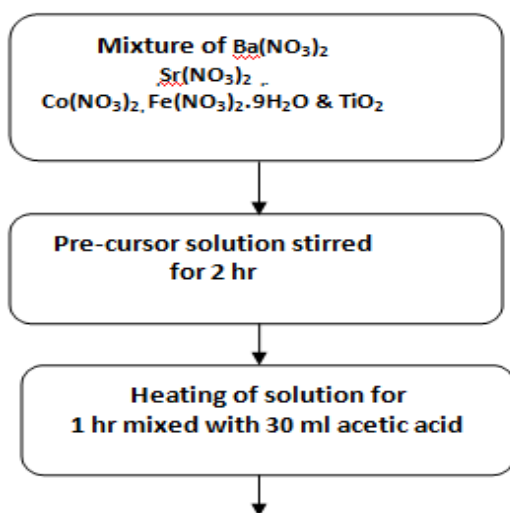
2. Experimental:

2.1.1 Materials:

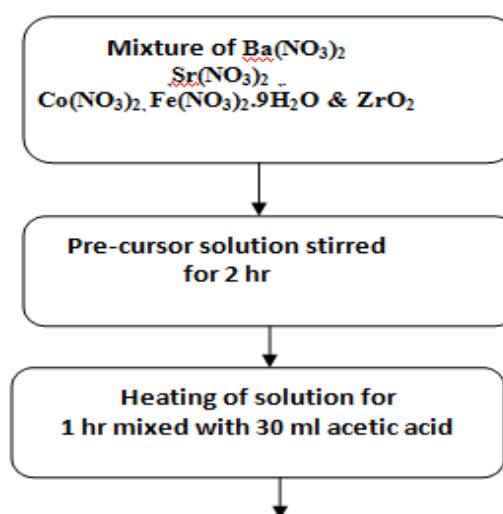
Commercial powders of AR grade of Aldrich Company were used in this work for the preparation of cathode. Ethylene di-amine-tetra-acetic acid (EDTA), ethylene glycol, Acetic acid, nitrate salts of Barium, Strontium, Cobalt, Iron, Titanium oxide and Zirconium oxide were purchased from Sigma Aldrich, USA. Ammonia solution is used as base. In the present observations, the Nano crystalline cathode material of Ba_{0.5} Sr_{0.5} (CO_{0.8}Fe_{0.2})_{1-x}Ti_xO_{3-δ} (BSCFTi) & Ba_{0.5} Sr_{0.5} (CO_{0.8}Fe_{0.2})_{1-x}Zr_xO_{3-δ} (BSCFZr) by varying x values, (x = 0, 0.10, 0.15, 0.20) BSCF Ti(5582Ti) and BSCFZr(5582Zr) powders were prepared by sol-gel process as it is one of the economical ways and characterizations like SEM/ EDAX, XRD TGA/DTA, Impedance Analyzer were used. Barium nitrate Ba(NO₃)₂, Strontium Nitrate Sr(NO₃)₂, Cobaltous Nitrate Co(NO₃)₂, Fluka Fe(NO₃)₂.9H₂O, TiO₂, ZrO₂ are used. Precursor solution is prepared by taking above powders by appropriate formula and mixing, aqueous solution of the above chemicals in molar ratio of 0.5:0.5 and 0.8:0.2 & required Acetic acid, ammonia, are added and c/n ratio is maintained as 0.5. The solution is taken in borosil glass beaker and placed on a Magnetic stirrer with hot plate for about 4 hr with appropriate speed and by heating at about 80°C to 100°C, the solution is stirred till it becomes like a gel and then, the speed is reduced, heated for some time till it becomes ash after burning. The ash is calcined first at 750°C, for 8 hr, and at 900°C, for 6 hr and at 1050°C, 1100°C each for 2hr.

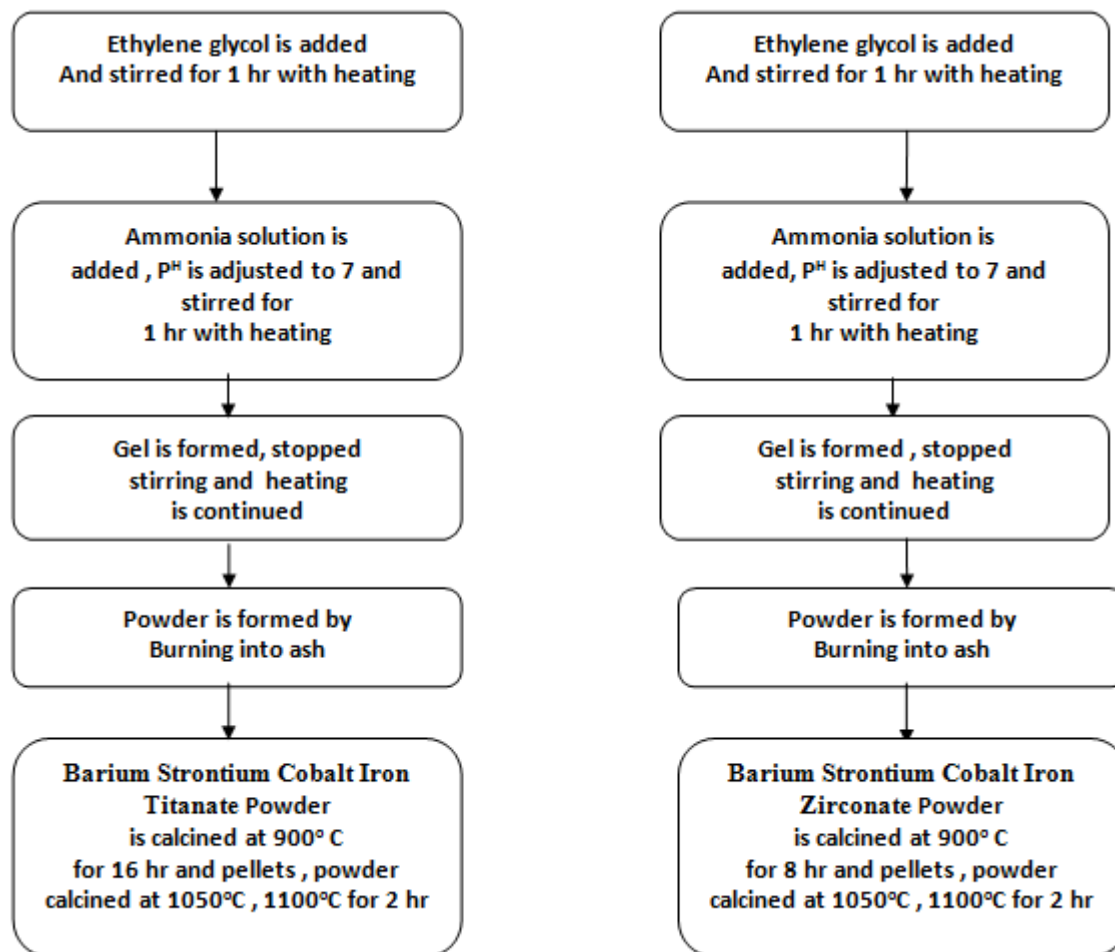
2.1.2 FLOW CHARTS OF PREPERATION OF SAMPLES:

i) Barium Strontium Cobalt Iron Titanate



ii) Barium Strontium Cobalt Iron Zirconate





3.Characterization

3.1 XRD Characterization:

X-ray diffraction (XRD) analysis of the sintered samples is carried out with XRD at 40 KV and 30mA, using $\text{CuK}\alpha$ radiation with diffraction angle (2θ) range from 20° to 80° and particle size is determined by line broadening technique as shown below for all four samples. It is clear that, powder is partially amorphous and it is observed that calcined powders were of Perovskite structure and these were found to be similar with other XRD's of various authors. It is observed that, at higher temperatures, the noise in XRD is reduced and still it can be reduced by calcining the samples at about 1100°C , 1150°C or more.

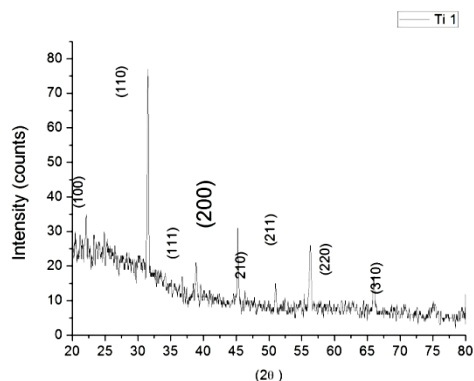


Figure1(a) XRD Pattern of $\text{Ba}_{0.5}\text{Sr}_{0.5}(\text{Co}_{0.8}\text{Fe}_{0.2})_{1-x}\text{Ti}_x\text{O}_{3-\delta}$ with $\delta=0$, $x=0.1$ calcined at 900°C

Table 1.Cathode (BSCFTi – 5582Ti)powders by sol-gel process.

Sample	Cathode powder	c/n
Ti ₁	Ba _{0.5} Sr _{0.5} [Co _{0.8} Fe _{0.2}] _{0.9} Ti _{0.1} O ₂	0.5
Ti ₂	Ba _{0.5} Sr _{0.5} [Co _{0.8} Fe _{0.2}] _{0.85} Ti _{0.15} O ₂	0.5
Zr ₁	Ba _{0.5} Sr _{0.5} [Co _{0.8} Fe _{0.2}] _{0.9} Zr _{0.1} O ₂	0.5
Zr ₂	Ba _{0.5} Sr _{0.5} [Co _{0.8} Fe _{0.2}] _{0.85} Zr _{0.15} O ₂	0.5

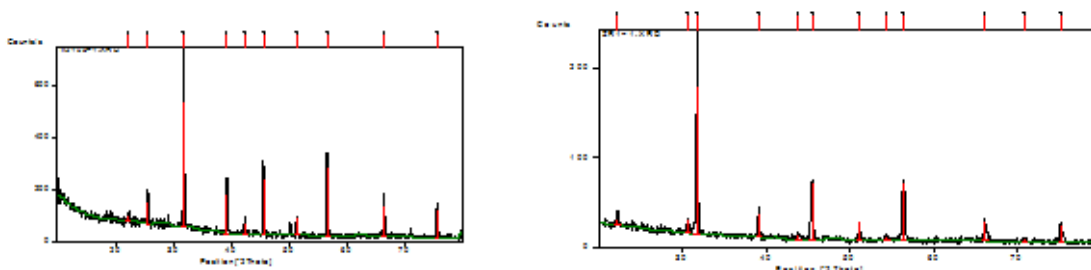


Figure1(b) XRDs of Ba_{0.5} Sr_{0.5} (Co_{0.8} Fe_{0.2})_{1-x} Ti_xO_{3-ε} with, x=0.1 & Ba_{0.5} Sr_{0.5} (Co_{0.8} Fe_{0.2})_{1-x} Zr_xO_{3-ε} with x=0, (calcined at 1050 °C)

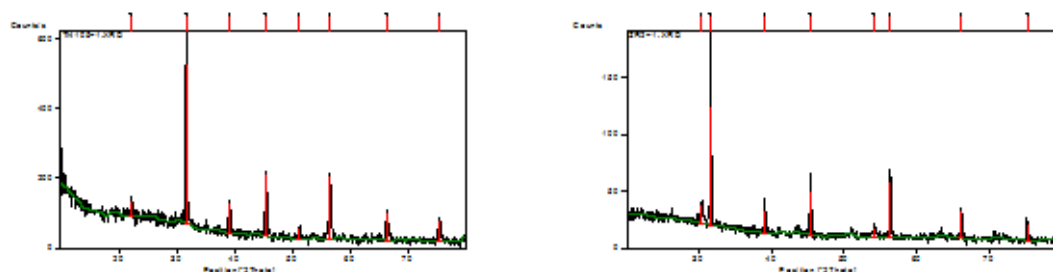


Figure2. XRDs of Ti₄ Ba_{0.5} Sr_{0.5} (Co_{0.8} Fe_{0.2})_{1-x} Ti_xO_{3-ε} (With X=0.2) & Zr₂ Ba_{0.5} Sr_{0.5} (Co_{0.8} Fe_{0.2})_{1-x} Zr_xO_{3-ε} (With X=0.1)samples, (calcined at 1050 °C)

3.2 SEM Characterization:

Few amounts of powders and pellets were used for study of compounds present in the samples after calcinations using ZEISS Scanning Electron microscope and images of various magnifications were done. The SEM with EDAX photographs of Ti1 & Ti2, Zr1 & zr2 samples are as under.

Ti1

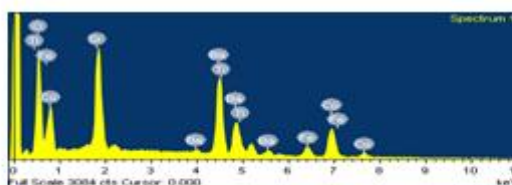


Figure 3(a)

Ti2

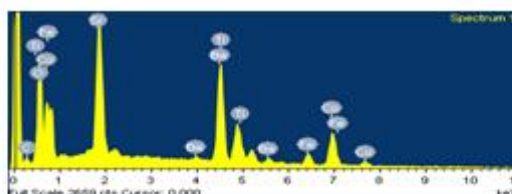
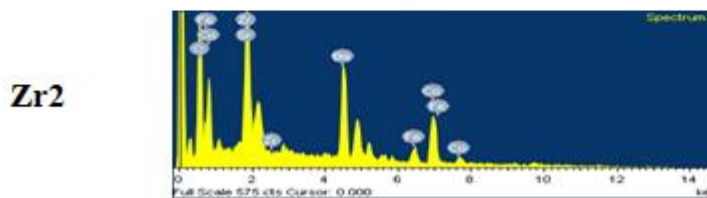
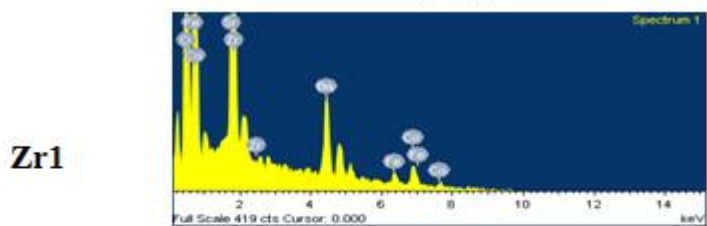
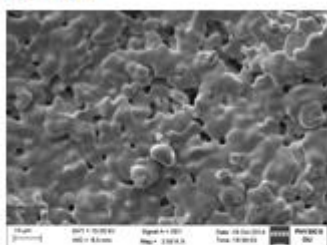


Figure 3(b)



SEM Photographs of Ti & Zr Samples

Ti1 (a)



Ti1 (b)

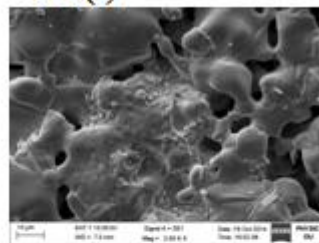
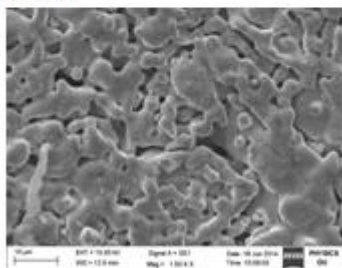


Figure 4(a)

Zr1(a)



Zr1 (b)

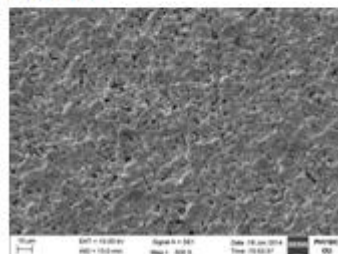
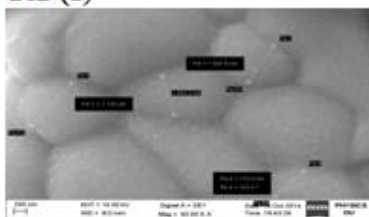


Figure 4(b)

Ti2 (a)



Ti2 (b)

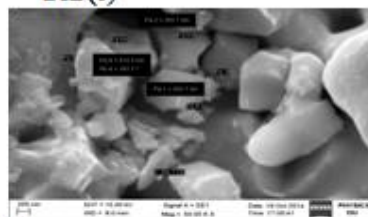
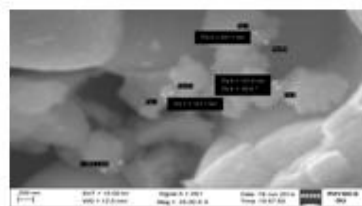


Figure 4(c)

Zr2(a)



Zr2 (b)

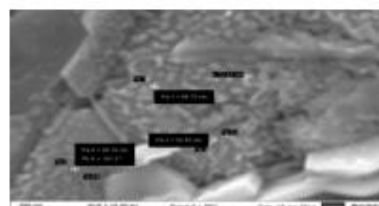


Figure 4(d)

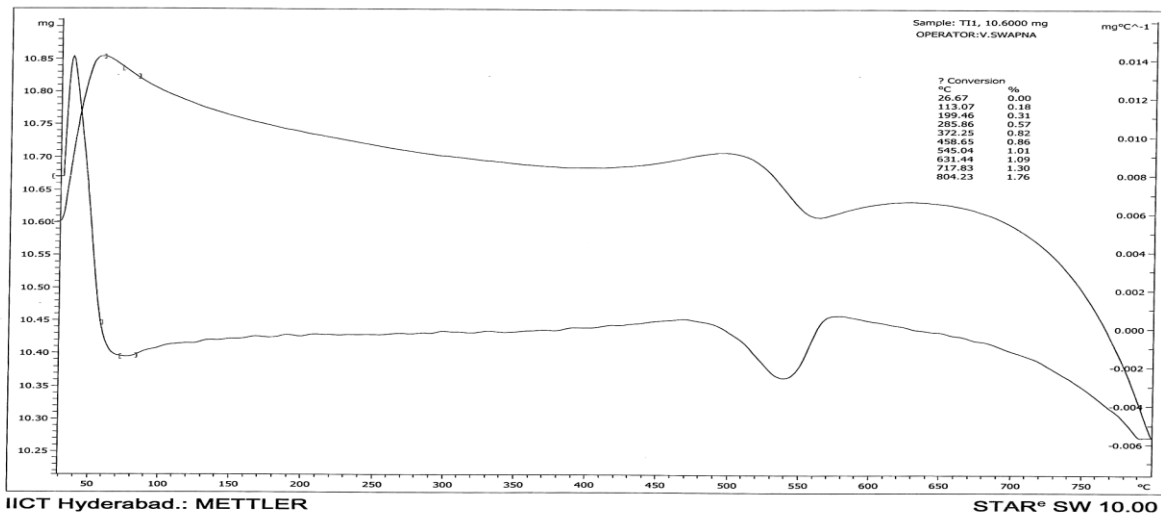
From SEM with EDAX analysis , it is found that the atomic percentage as taken in the formula is not changed and all atoms are present in the same proportion , particle sizes are noted which are in good coincidence with the data taken from XRD .

The figures show the presence of Ba, Sr, Co, Fe, Ti, Zr & C peaks. The appearance of C may be due to usage of acetic acid. This C % has been reduced by calcining the samples at a higher temperature.

4. TGA/DTA Characterization:

The curves in figures 5(a) ,5(b) 5(c) & 5(d) correspond to TGA (weight loss in % Vs temperature) and DTA(Rate of loss of weight Vs temperature) for Ti₁, Ti₂ & Zr₁ ,Zr₂ samples.DTA is studied with difference in temperature and flow of heat between the sample and a reference. Moisture, Thermal stability and composition are studied simultaneously by TG/DTA referring Exothermic and Endothermic processes.

Powder samples of Ti₁of 10.6 mg and Ti₂of 7.6 mg, Zr₁ of 8.3 mg and Zr₂ of 10.9 mg are taken and corresponding curves are recorded. The weight loss is observed for three times in TGA first at 78 ° C due to evaporation of moisture , second at 490 ° C due to evaporation of nitrates and third at 640 ° C due to evaporation of other impurities because of usage of acids, bases etc.,. The melting point can be at about 1070 °C or 1100 ° C.



Temperature (X-Axis), Weight loss in% (Y-Axis)
Figure. 5(a) TGA/DTA Curves for Ba_{0.5}Sr_{0.5}[Co_{0.8}Fe_{0.2}]_{0.9}Ti_{0.1}O₂

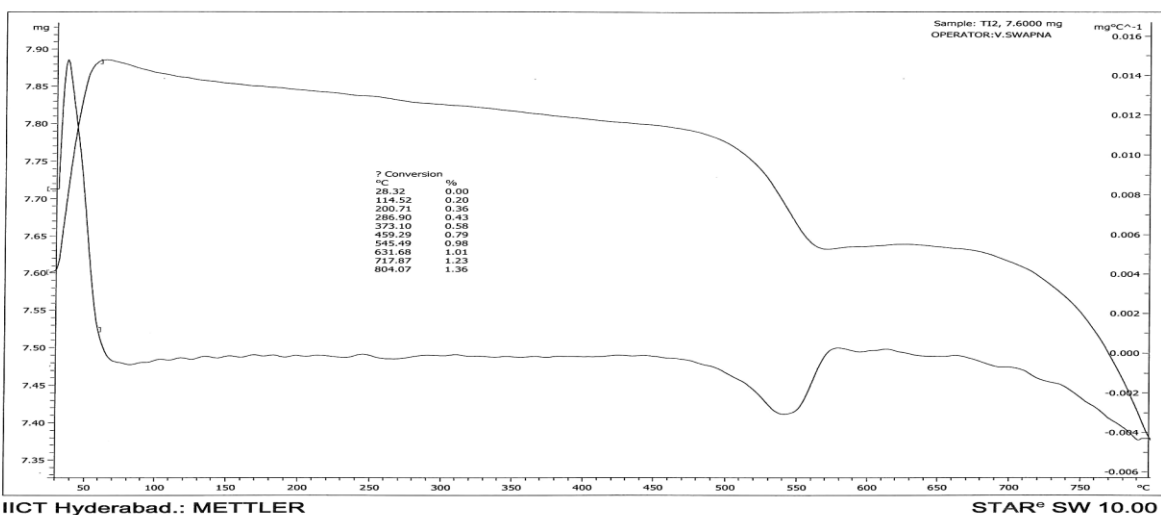
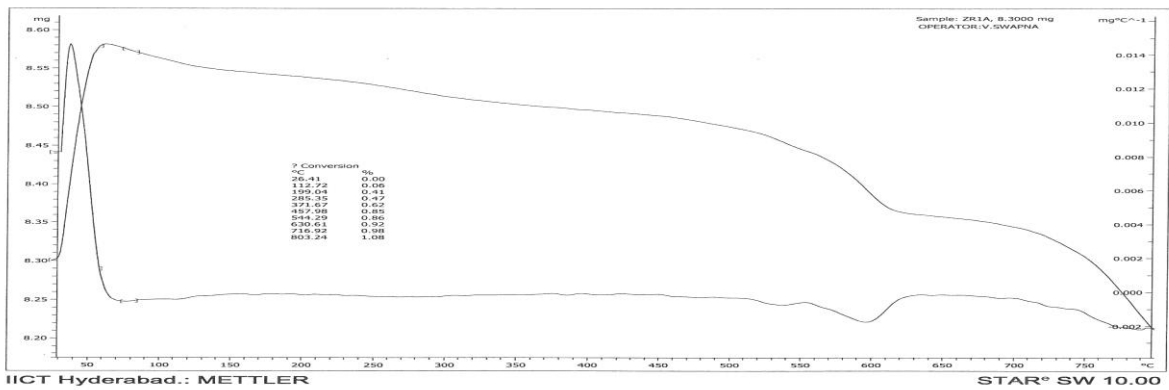
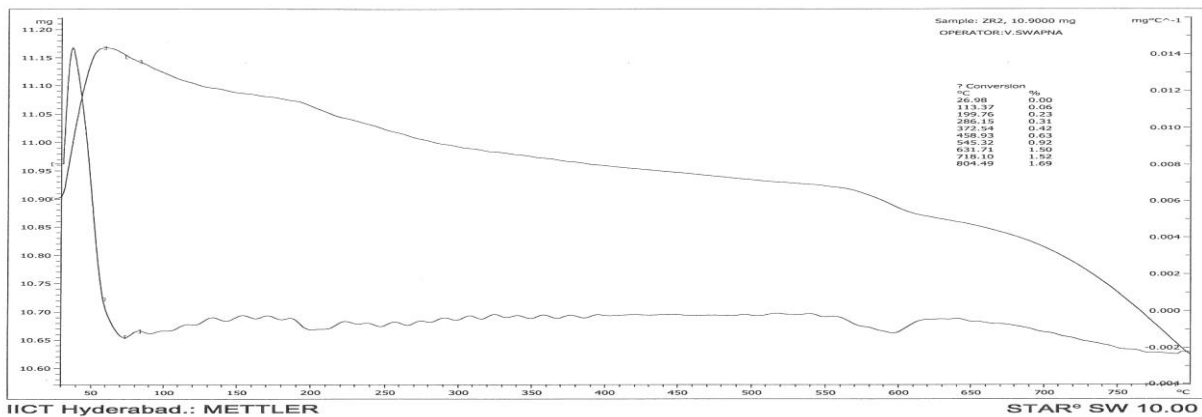


Fig. 5(b)TGA/DTA Curves for Ba_{0.5}Sr_{0.5}[Co_{0.8}Fe_{0.2}]_{0.85}Ti_{0.15}O₂
 Temperature (X-Axis), Weight loss in% (Y-Axis)



Temperature (X-Axis), Weight loss in % (Y-Axis)
 Figure. 5(c) TGA/DTA Curves for Ba_{0.5}Sr_{0.5}[Co_{0.8}Fe_{0.2}]_{0.9}Zr_{0.1}O₂



Temperature (X-Axis), Weight loss in % (Y-Axis)
 Fig. 5(d) TGA/DTA Curves for Ba_{0.5}Sr_{0.5}[Co_{0.8}Fe_{0.2}]_{0.85}Zr_{0.15}O₂

5. Impedance Analysis:

To characterize the electrochemical properties of BSCFTi cathode, AC impedance values are measured and characterization of cathode processes is based on the application of ac potential

$$E(t) = E_0 \cos(\omega t + \phi) \text{ ----- (1)}$$

of minimum amplitude such that ac current $I(t) = I_0 \cos(\omega t - \phi) \text{ ----- (2)}$

is obtained. Impedance, $Z = \frac{E(t)}{I(t)} \text{ ----- (3)}$ is calculated at different AC frequencies up to few

MHz. The impedance measurements characterize the physical and chemical processes related to time constants, electron transfer at high frequencies and mass transfer at low frequencies.

In the present study, the impedance measurements were carried from room temperature to 150⁰ C and Nyquist plots ($Z_s = Z_{Real} + Z_{Imaginary}$) are drawn as shown in figures 7(a) for Ti₁ sample and 8(a) for Ti₂ sample respectively.

The Cole-Cole plots are observed for Z^I and Z^{II} plots are as depicted in figures 7(a) & 8(a).

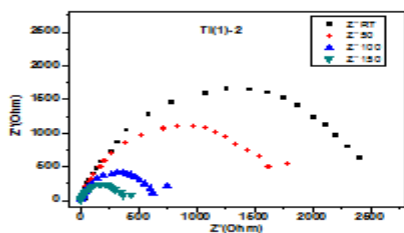


Figure .7(a) COLE-COLE plot of Ti₁ sample

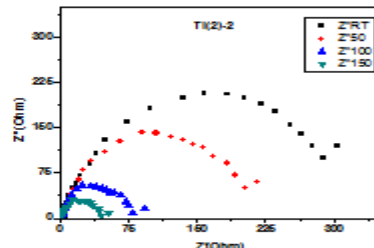


Figure .7(b) COLE-COLE plot of Ti₂ sample

The stable behavior of the real part of the impedance with frequency is observed with increase of temperature as shown in figures 8(a) & 8(b).

From cole-cole plots one can calculate the grain resistance (R_g) and grain boundary (R_{gb}) resistance and their temperature dependence can be observed.

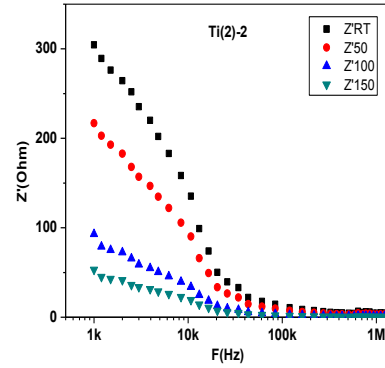
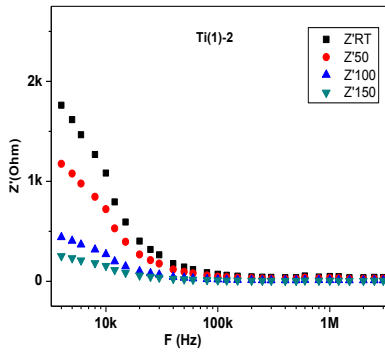


Figure.8 (a) Z Vs Frequency curves for Ti_1 sample

Figure.8 (b) Z Vs Frequency curves for Ti_2 sample

It is observed from figures 9 (a) and 9(b) that, the peak frequencies were shifted for imaginary component of Z'' as temperature increases. This is the relaxed behavior of a sample.

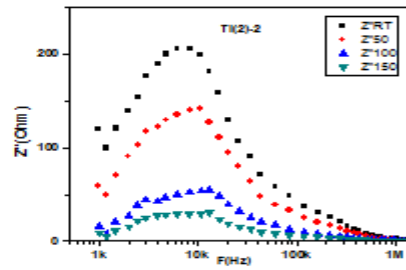
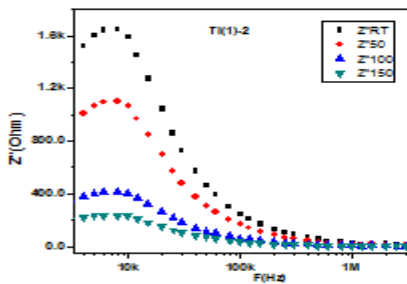


Figure.9(a) Z Vs Frequency curves for Ti_2 Sample

Figure.9 (b) Z Vs Frequency curves for Ti_1 Sample

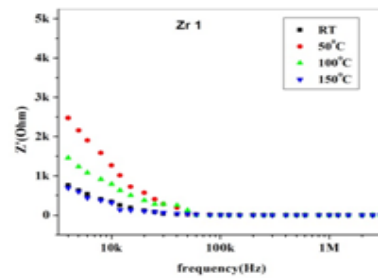
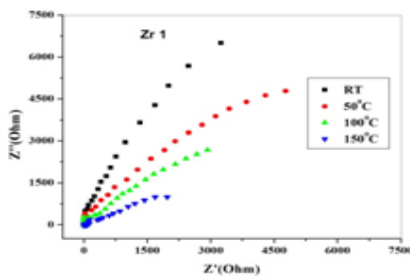


Fig. 10(a) Z' Vs Z'' of Zr_1 Sample

10(b) Frequency Vs Z' of Zr_1 Sample

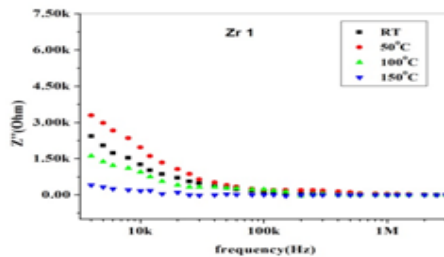


Fig. 10(c) Z' Vs Z'' of Zr_1 Sample

AC conductivity is calculated by the formula $\sigma_{AC}^I = \frac{Y^I t}{A}$ where Y^I is called admittance, t is thickness of the sample and A is area of the sample. The conductivities are tabulated in tables 2 & 3 below.

Table 2. Calculation of conductivities of Ti₁ Sample:

S.No	Temperature Deg C	Resistance (ohm)	Admittance (Y) (Mhos)	Area (A) m ²	Thickness(t) m	$\sigma_{AC}^I = \frac{Y^I t}{A}$ S/m
1	Room temp.	1750	5.714×10^{-4}	69.42×10^{-6}	1.46×10^{-3}	0.0120
2	50	1200	8.33×10^{-4}	69.42×10^{-6}	1.46×10^{-3}	0.01752
3	100	500	2×10^{-3}	69.42×10^{-6}	1.46×10^{-3}	0.042059
4	150	250	4×10^{-3}	69.42×10^{-6}	1.46×10^{-3}	0.08411

Table 3. Calculation of conductivities of Ti₂ Sample:

S.No	Temperature Deg C	Resistance (ohm)	Admittance (Y) (Mhos)	Area (A) m ²	Thickness(t) m	$\sigma_{AC}^I = \frac{Y^I t}{A}$ S/m
1	Room temp.	320	3.125×10^{-3}	70.6124×10^{-6}	1.42×10^{-3}	0.06284
2	50	230	4.347×10^{-3}	70.6124×10^{-6}	1.42×10^{-3}	0.087417
3	100	95	0.01052	70.6124×10^{-6}	1.42×10^{-3}	0.211556
4	150	50	0.02	70.6124×10^{-6}	1.42×10^{-3}	0.402197

Note: Similar changes in conductivities were observed for Zr₁ & Zr₂ samples.

6. Results and Discussions:

- In this study, the composition of the material was adjusted in such a way that the dopant will take its place on site B of Perovskite structure ABO₃.
- The X-Ray diffraction patterns of powdered BSCFTi & BSCFZr were studied at different temperatures starting from 750^oC but diffraction peaks were found to be broad and very weak and sample was not crystallized perfectly. But, as the sintering temperature is increased, the impurity peaks due to Fe₃O₄Co. The sharp lines in XRD pattern depicts a well crystallized structure is formed. All the peaks indicate a Perovskite structure and correspond to planes (100), (110), (111), (200), (210), (211), (220), (300), (221), (310). There are some other peaks are also observed due to impurities and these were also disappeared as the doping of Ti is increased and sintering is done for much time accordingly. The particle sizes of samples are calculated using XRD data.
- Densities of samples are calculated and for all samples the density percentage is above 90% .
- SEM images of BSCFTi & BSCFZr proved the presence of porous spherical particles of nano size for the powders calcined above 850^oC.
- From TGA plots it can be concluded that there is no weight loss after about 540^oC which indicates that combustion process is completed at this temperature and oxide phases are formed.
- As the concentration of Ti increases the resistance of the sample has been decreased and conductivity increased.
- AC conductivities of all samples are calculated and observed that, as temperature is increased, resistance is decreased and conductivity is increased .

7. Acknowledgements:

Authors thank R&D team of St. Mary's Engineering College, Department of Physics - Osmania University, and Department of physics-JNTU Hyderabad, Chairman, Secretary, Principal & Department Of Physics-Visvesvaraya College of Engineering and Technology, Hyderabad and ICT, HYDERABAD.

References

- [1]. T. Ishihara, H. Matsuda, Y. Takita, J. Am. Chem. Soc. 116(1994) 3801
- [2]. K. Huang, M. Feng, J.B. Goodenough, J. Electrochem. Soc.
- [3]. J.P.P. Hujismans, F.P.F. Berkel, G.M. Christie, J. Power

- [4]. R. Maric, S. Ohara, T. Fukui, H. Yoshida, M. Nishimura, T. Vol. PV 94-12, Electrochemistry Society, 1994, Inagaki, K. Miura, J. Electrochem. Soc. 146 2006
- [5]. P. Huang, A. Horko, A. Petric, J. Am. Ceram. Soc. 82 (1999) Electrochem. Soc. 134 (1978) 21412402
- [6]. F. Chen, M. Liu, J. Solid State Electrochem. 3 (1998) 7. Tuller (Eds) Proceeding 1st International Symposium Ionic
- [7]. T. Ishihara, H. Matsuda, Y. Takita, in: Proceedings 2nd Ionic and Mixed Conducting Ceramics, Electrochemistry Society, and Mixed Conducting Ceramics, Vol PV 94-12, Electro- 1991, p. 122. Chemistry Society, 1994, p. 85.
- [8]. T. Ishihara, M. Honda, Y. Takita, Recent Res. Dev. Electrochem 2 (1999) 15
- [9]. N.Q. Minh, T. Takahashi, in: Science and Technology of Nishiguchi, Y. Takita, J. Electrochem. Soc. 145 (1999) 3177. Ceramic Fuel Cell, 1995, p. 147.
- [10]. S. Majumdar, T. Claar, B. Flandermeyer, J. Am. Ceram. Soc. 144 (1997) 3620. 69
- [11]. O. Yamamoto, Y. Takeda, R. Kanno, H.U. Anderson, Solid State Ionics 22 (1989)
- [12]. A. Hammouche, E. Siebert, A. Hammou, Mater. Res. Bull. 24 (1989) 367.
- [13]. T. Ishihara, M. Honda, T. Shibayama, H. Minami, H. Nishiguchi, Y. Takita,
- [14]. J. A. Kilner, R.A. De Souza, I. C. Fullerton, Solid state Ionics P. SSC 86-88 (1996) 703. O2
- [15]. A Boudghene Stambouli and E. Traversa, Renewable and Suitable Energy Rev., 6.433 (2002)
- [16]. S. J. Skinner, Jnt. T. Inorganic Matter., 3, 113 (2001)
- [17]. Z. Shao and S. M. Haile, Nature (London) 431, 432, 170 (2004)
- [18]. Y. Itoh V, Nishida, A. Tomita, Y. Fujie. Solid state communication. 149. 41 (2008)
- [19]. B. Liu, Y. Zhang and L. Tang, Int. J. Hydrogen Energy, 34, 435 (2009)
- [20]. X. Sun, S. Li, J. Sun, X. Liu, B. Zhu, Int. J. Electrochem. Sci. (2007) 462
- [21]. A. Subrahmanya, T. Saradha, S. Muzumathi, J. Power Sources 165 (2007) 728
- [22]. H. Zhao, F. Mauvy, C. Lalanne, J.M. Bassat, S. Fourcade, J.C Grenier, Solid State Ionics 179 (2008) 2000
- [23]. A. Princivalle, E. D. Jurado, SSI 179 (2008) 1921
- [24]. V. B. Vert, J.M. Serra, Fuel Cells (2009) 663
- [25]. Y. Li, R. Gemmen, X. Liu, J. Power sources, 195 (2010) 3345 [26] S.S. Shimizu, T. Yamaguchi, Y. Fujishiro, ECS Tans. 25 (2009) 975